AEC DISTRIBUTION FOR PART 50 DOCKET MATERIAL
(TEMPORARY FORM)

CONTROL NO: 6284

FILE:

FROM:	DATE OF DOC	DATE REC'D	LTR	MEMO	RPT	OTHER
Carolina Power & Light Company Raleigh, N. C. 27602 E. E. Utley	8-14-73	8-16-73	X			

TO:	ORIG	CC	OTHER	SENT AEC PDR	SENT LOCAL PDR
Mr. Schemel	3 signed			X	X

CLASS	UNCLASS	PROP INFO	INPUT	NO CYS REC'D	DOCKET NO:
				40	50-261

DESCRIPTION:
Ltr re our 8-3-73 ltr, trans the following:

ENCLOSURES:
ATTACHMENT I - Additional Info in Support of 100% Thermal Power Authorization & Tech Specs Modifications.

(40 cys rec'd)

ACKNOWLEDGED
Do Not Remove

PLANT NAME: H. B. Robinson Unit No. 2

FOR ACTION/INFORMATION 8-16-73 AB

BUTLER(L)	SCHWENCER(L)	ZIEMANN(L)	REGAN(E)
W/ Copies	W/ Copies	W/ Copies	W/ Copies
CLARK(L)	STOLZ(L)	DICKER(E)	
W/ Copies	W/ Copies	W/ Copies	W/ Copies
GOLLER(L)	VASSALLO(L)	KNIGHTON(E)	
W/ Copies	W/ Copies	W/ Copies	W/ Copies
KNIEL(L)	✓SCHEMEL(L)	YOUNGBLOOD(E)	
W/ Copies	W/ 9Copies	W/ Copies	W/ Copies

INTERNAL DISTRIBUTION

✓REG FILE	TECH REVIEW	DENTON		A/T IND
✓AEC PDR	HENDRIE	GRIMES	LIC ASST	BRAITMAN
✓OGC, ROOM P-506A	SCHROEDER	GAMMILL	DIGGS (L)	SALTZMAN
✓MUNTZING/STAFF	MACCARY	KASTNER	GEARIN (L)	
CASE	KNIGHT	BALLARD	GOULBOURNE (L)	PLANS
GIAMBUSSO	PAWLICKI	SPANGLER	LEE (L)	MCDONALD
BOYD	SHAO		MAIGRET (L)	✓DUBE
MOORE (L)(BWR)	STELLO	ENVIRO	SERVICE (L)	
DEYOUNG(L)(PWR)	HOUSTON	MULLER	SHEPPARD (E)	INFO
✓SKOVHOLT (L)	NOVAK	DICKER	SMITH (L)	C. MILES
P. COLLINS	ROSS	KNIGHTON	✓TEETS (L)	
	IPPOLITO	YOUNGBLOOD	WADE (E)	
REG OPR	TEDESCO	REGAN	WILLIAMS (E)	
✓FILE & REGION(3)	LONG	PROJECT LDR	WILSON (L)	
MORRIS	LAINAS			
STEELE	BENAROYA	HARLESS		
	VOLLMER			

EXTERNAL DISTRIBUTION

✓1 - LOCAL PDR Hartville, S. C.	(1)(2)(10)-NATIONAL LAB'S	1-PDR-SAN/LA/NY
✓1 - DTIE(ABERNATHY)	1-R.Schoonmaker,OC,GT,D-323	1-GERALD LELLOUCHE
✓1 - NSIC(BUCHANAN)	1-R. CATLIN, E-256-GT	BROOKHAVEN NAT. LAB
1 - ASLB(YORE/SAYRE/ WOODARD/"H" ST.	1-CONSULTANT'S NEWMARK/BLUME/AGBABIAN	1-AGMED(WALTER KOESTER RM-C-427-GT
✓16 - CYS ACRS ~~HOLDING~~ SENT TO LIC ASST. S. TEETS ON 8-16-73	1-GERALD ULRIKSON...ORNL	1-RD..MULLER..F-309 GT

Regulatory File Cy.

CP&L

Carolina Power & Light Company

August 14, 1973

File: NG 5211.1

Serial: NG-73-285

Mr. Robert J. Schemel, Chief
Operating Reactors Branch #1
Directorate of Licensing
U. S. Atomic Energy Commission
Washington, D. C. 20545

50-261

Dear Mr. Schemel:

H. B. ROBINSON UNIT NO. 2
LICENSE DPR-23
ADDITIONAL INFORMATION IN SUPPORT OF 100% THERMAL POWER
AUTHORIZATION AND TECHNICAL SPECIFICATION MODIFICATIONS

In your letter of August 3, 1973, you requested that additional information be supplied to further understand our request of July 6, 1973, for use of the $\bar{R}$ technique to correlate axial flux traverses in each instrument thimble and the core heat flux nuclear hot channel factor instead of the technique using the bounding value of F_{xy} in conjunction with the axial power distribution. You also requested that additional information which was discussed in our July 18, 1973, meeting be documented in the public record and that Technical Specification changes to incorporate the use of the $\bar{R}$ method be supplied.

The responses to your request for additional information are included as Attachment 1 and follow in the same order as in your request. The changes to the Technical Specifications are incorporated in Attachment 2, and provide for the use of the $\bar{R}$ method. In addition, further clarifications have been incorporated in other sections dealing with power distribution monitoring to provide consistency with present Technical Specifications for other plants.

DBW:mvp

Very truly yours,

E. E. Utley
Vice-President
Bulk Power Supply

Attachments

cc: Messrs. N. B. Bessac
C. D. Barham
B. J. Furr
D. V. Menscer
D. B. Waters

6284

336 Fayetteville Street • P. O. Box 1551 • Raleigh, N. C. 27602

ATTACHMENT I
ADDITIONAL INFORMATION REQUESTED IN LETTER OF AUGUST 3, 1973
H. B. ROBINSON UNIT NO. 2
DOCKET NO. 50-261

1. In order to compare the $\bar{R}$ and F_{xy} methods of correlating axial power distribution to F_q^N, eleven of the most recent full core movable detector maps (designated as Maps 102-112), which were obtained at power levels in excess of 70% power, were analyzed. Based on these maps and the $\bar{R}$ analysis presented in our letter of July 6, 1973, (which spanned Maps 102-108), four thimbles were selected for investigation. These thimbles met the following two conditions: 1) The value of the measured axial peaking factor, $F_{z\,\text{measured}}$, was at least as large as the value of the average core axial peaking factor, $\bar{F}_z$; based on a peak in the top of the core; 2) the calculated values of $\bar{R}$ for the thimbles, based on the Maps 102-108, had a standard deviation (σ) of approximately 2%. The value of F_{xy} limiting for each map was determined by the ratio of F_q^N and the value of the average axial peaking factor in the plane of F_q^N (not necessarily the peak, $\bar{F}_z$). The analysis was based on the peak occurring in Regions 2 and 3, which is the most limiting region as shown in our letter of August 1, 1973.

Based on the above conditions, calculations of F_q^N using the $\bar{R}$ and F_{xy} methods were performed, and a comparison was made with the measured values obtained from the full core movable detector map by computing the percentage deviation between the measured and the computed values, defined as:

$$\Delta\% = \left(\frac{F_{q\ \text{measured}}^N - F_{q\ \text{calculated}}^N}{F_{q,\ \text{calculated}}^N}\right) \times 100$$

In addition, the standard deviation, σ, was computed for each thimble and each of the two methods. The results of the above calculations are presented in Table 1. In general, the two methods give similar results as far as overpredicting or underpredicting $F_{q\ \text{measured}}^N$ for a particular map. The standard deviation in three out of four thimbles investigated was higher

for the F_{xy} method than for the $\bar{R}$ method, and was essentially identical in the fourth thimble. Use of a statistical approach is consistent with the uncertainty value assigned to a full-core map (5%), and provides an additional degree of conservatism to the assurance that F_q^N is less than the limiting value in the core. The maximum deviation in a non-conservative direction for all of the calculations is 4.33% for the F_{xy} method and 4.39% for the $\bar{R}$ method (Map 104, Thimble F-4).

Although the two methods provide similar results, as expected, Carolina Power & Light Company still recommends the use of the $\bar{R}$ method as a more consistent approach to following the variation of F_q^N over a wide range of power distributions and power levels. One example of this is the calculations for Maps 111 and 112; the F_{xy} method consistently underpredicts F_q^N in comparison with the $\bar{R}$ method. Also, the ability to select any thimble and relate it to $F_{q\ \text{measured}}^N$ allows additional freedon in the selection of thimbles and detectors for surveillance, and, as has been shown above, is consistent with other more established methods of relating axial and radial power distributions to the peak heat flux in the reactor core.

MAP No.

	102	103	104	105	106	107	108	109	110	111	112	
F_q^N measured	1.637	1.881	1.783	1.611	1.537	1.498	1.523	1.528	1.509	1.470	1.498	Thimble F-4
① $F_{xy} \cdot F_{zi}$ measured	1.669	1.903	1.709	1.611	1.532	1.535	1.496	1.561	1.537	1.440	1.470	
② $\bar{R} \cdot F_{zi}$ measured	1.690	1.894	1.708	1.614	1.535	1.523	1.505	1.560	1.547	1.509	1.550	
① Δ%	-1.95	-1.17	+4.33	0	+0.33	-2.41	+1.80	-2.11	-1.82	+2.08	+1.90	σ=2.11
② Δ%	-3.14	-0.69	+4.39	-0.18	+0.13	-1.64	+1.19	-2.05	-2.45	-2.58	-3.35	σ=2.37

F_q^N measured	1.637	1.881	1.783	1.611	1.537	1.498	1.523	1.528	1.509	1.470	1.498	Thimble L-6
① $F_{xy} \cdot F_{zi}$ measured	1.689	1.974	1.766	1.650	1.600	1.572	1.488	1.593	1.587	1.429	1.454	
② $\bar{R} \cdot F_{zi}$ measured	1.670	1.919	1.723	1.614	1.565	1.523	1.461	1.555	1.559	1.461	1.496	
① Δ%	-3.07	-4.71	+0.96	-2.36	-3.94	-4.71	+2.35	-4.08	-4.91	+2.87	+3.03	σ=3.56
② Δ%	-1.98	-1.98	+2.90	-0.18	-1.79	-1.64	+4.24	-1.74	-3.21	+0.62	+0.13	σ=2.21

F_q^N measured	1.637	1.881	1.783	1.611	1.537	1.498	1.523	1.528	1.509	1.470	1.498	Thimble L-9
① $F_{xy} \cdot F_{zi}$ measured	1.690	1.971	1.771	1.643	1.573	1.545	1.502	1.600	1.577	1.452	1.499	
② $\bar{R} \cdot F_{zi}$ measured	1.677	1.923	1.734	1.612	1.544	1.503	1.479	1.567	1.552	1.490	1.548	
① Δ%	-3.14	-4.56	+0.67	-1.95	-2.29	-3.04	+1.40	-4.50	-4.31	+1.24	-0.07	σ=2.89
② Δ%	-2.38	-2.18	+2.82	-0.06	-0.45	-0.33	+2.97	-2.49	-2.77	-1.34	-3.23	σ=2.21

F_q^N measured	1.637	1.881	1.783	1.611	1.537	1.498	1.523	1.528	1.509	1.470	1.498	Thimble D-10
① $F_{xy} \cdot F_{zi}$ measured	1.684	1.947	1.764	1.646	1.589	1.568	1.499	1.610	1.639	1.424	1.443	
② $\bar{R} \cdot F_{zi}$ measured	1.671	1.900	1.727	1.615	1.561	1.524	1.477	1.577	1.616	1.461	1.490	
① Δ%	-2.79	-3.39	+1.08	-2.13	-3.27	-4.46	+1.60	-5.09	-7.93	+3.23	+3.81	σ=3.95
② Δ%	-2.03	-1.00	+3.24	-0.25	-1.54	-1.71	+3.11	-3.11	-6.62	+0.62	+0.54	σ=2.78

Axial Offset (%)	+5.83	+15.88	-18.31	+2.21	-0.41	-2.03	-5.20	-0.55	-1.24	-5.27	-7.83

2. A new S(Z) curve for region 4 has been constructed to allow for possible collapses in neighboring region 2 fuel assemblies. This curve is based on a detailed analysis of assembly-wise power distributions calculated for Carolina Power & Light Company, Cycle 2 by the PHASTR two-dimensional diffusion theory code. Beginning-of-cycle and end-of-cycle rodwise power distribution for region 4 assemblies which border region 2 assemblies (and could possibly contain the hot rod) were studied. The effect of a collapse in an outer row rod of a region 2 fuel assembly on the adjacent region 4 rods was compared to the effect of a gap in a region 4 rod next to the hot rod in the assembly. At beginning-of-cycle the maximum power achievable in the hot rod due to a gap in an adjacent rod is greater ($\sim$ 4%) than the power which can be achieved in an outer rod due to a collapse in an adjacent region 2 assembly. An end-of-cycle, however, the outer rod can be approximately 1% higher in power than the hot rod due to the same phenomena as at BOL due to power flattening with burnup. An increase in the power spike factor, S(Z), for region 4 of Cycle 2 is therefore recommended such that the hot rod is adequately predicted. Figure 1 shows the suggested curve.

This recommended curve provides good verification of the 1.15 value suggested by Carolina Power & Light Company for region 4 in memo NG-73-110[(2)]. In Figure 1 it can be seen that the value 1.15 agrees quite well with the 1.25 value for regions 2 and 3 at 120 inches elevation. On this basis, then, the default value of 1.15 for S(Z) in region 4 need not be increased by a factor of 1.01.

Figures 2 through 5 show the detailed rod-wise power distributions analyzed. Assemblies B9 and C11 (see core map in Carolina Power & Light DSAR for assembly coordinates) were identified as region 4 assemblies bordering region 2 assemblies (there are no region 3 assemblies bordering region 4 assemblies in Carolina Power & Light Cycle 2) which would be most affected by collapses in region 2 assemblies, since B9 and C11 (and their symmetric counterparts) could conceivably contain the hot rod. Both BOL and EOL cases were studied since burnup flattening of the power shape with lifetime was felt to be important.

The approach was simply to ascertain that the hot rod was always conservatively predicted, regardless of collapses or gaps. To do this, the power spike fractions shown in Figure 4.1 of the Carolina Power & Light Cycle 2 DSAR were utilized. The analysis is given on the next several pages. Power spike values from the top of the core were used since the result is not a function of elevation (i.e., the choice of elevation is arbitrary).

Assembly B9 at BOL

A. Effect of gap on hot rod in assembly (M6)

$1.3784 \times 1.164 = 1.6044$

↑ Region 4 with gaps

B. Effect of collapse in bordering region 2 fuel on hot rod in outer row of assembly (R6)

$1.2192 \times (1.263 \times 1.00) = 1.5398$

↑ Region 2 with collapses

C. Effect of gap on R6

$1.2192 \times 1.164 = 1.4191$

D. Effect of collapse in bordering region 2 fuel on hot rod in second to outer rod of assembly (P10)

$1.2898 \times \{1 + (1.263 - 1.0) \times .3\} = 1.3916$

E. Effect of gap on P10

$1.2898 \times 1.164 = 1.5013$

F. Effect of collapse in bordering region 2 fuel on hot rod in third to outer row of assembly (N9)

$1.3568 \times \{1 + (1.263 - 1.0) \times .13\} = 1.4032$

G. Effect of gap on N9

$1.3568 \times 1.164 = 1.5793$

From the above, it is concluded that cases C, E and G will always be less than case A. Collapses are only seen three pitches away and the hot rod is always four pitches into the assembly. For Figures 2 through 5, the following table is constructed.

Case	Rod A and power	Rod B and power	Rod D and power	Rod F and power
2	(M6) 1.6044	(R6) 1.5398	(P10) 1.3916	(N9) 1.4032
3	(L4) 1.6191	(K1) 1.5455	(K2) 1.3987	(J3) 1.4063
4	(M6) 1.5844	(R6) 1.5914	(P6) 1.4022	(J3) 1.3833
5	(L4) 1.5120	(K1) 1.5261	(K2) 1.3418	(J3) 1.3235

From case 4 $\frac{1.5914}{1.5844} = 1.0044$

From case 5 $\frac{1.5261}{1.5120} = 1.0093$

Therefore a 1% increase in S(z) for Region 4 fuel will mean that the hot rod power is always conservatively predicted.

FIGURE 1

POWER SPIKE VS ELEVATION

H. B. ROBINSON UNIT 2 - CYCLE 2

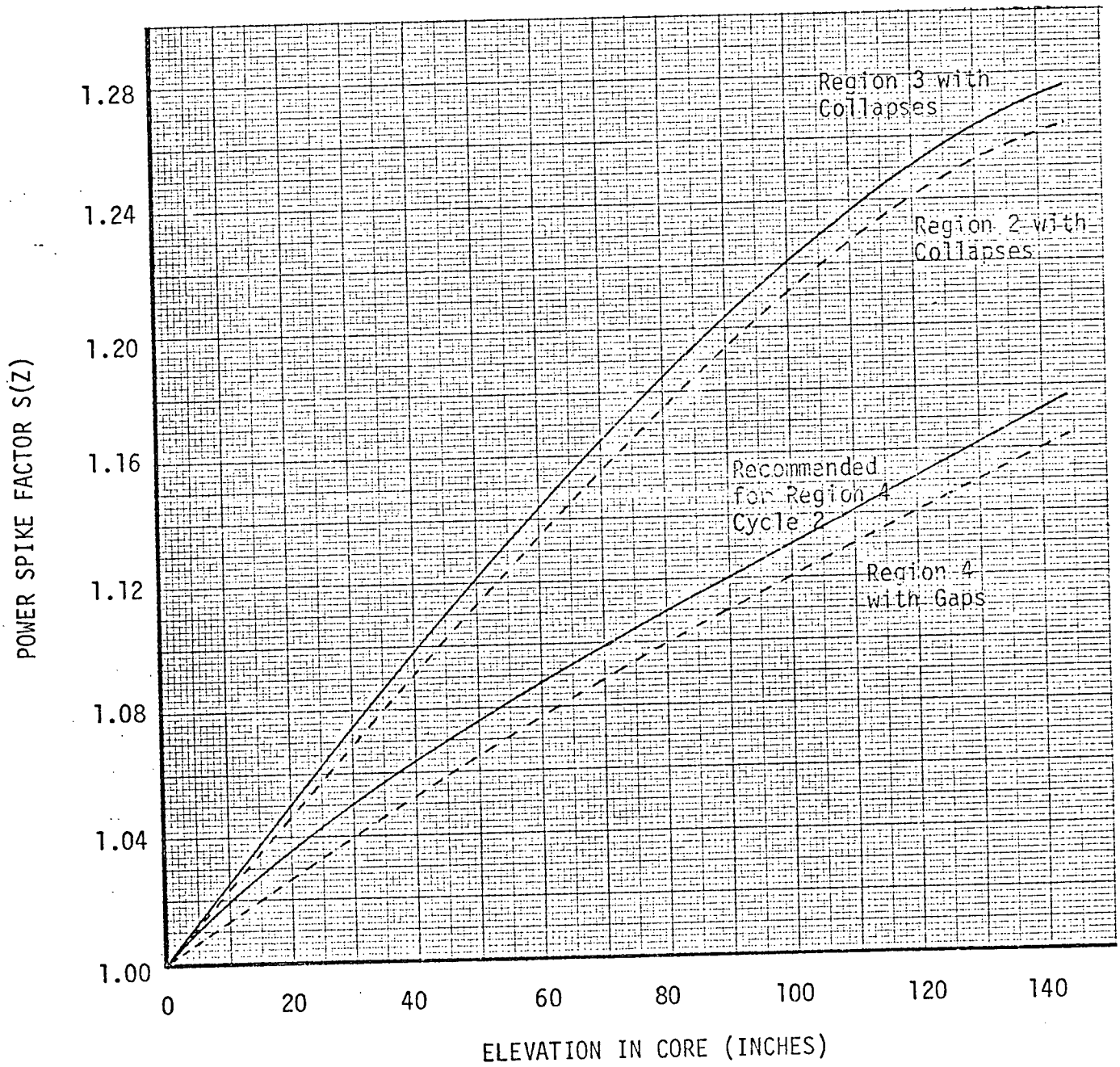

ASSEMBLY B9 BOL POWER DISTRIBUTION

	R	P	N	M	L	K	J	H	G	F	E	D	C	B	A
1	1.166	1.172	1.182	1.180	1.178	1.175	1.159	1.140	1.130	1.117	1.092	1.067	1.043	1.009	0.98
2	1.179	1.211	1.247	1.236	1.237	1.250	1.219	1.185	1.189	1.189	1.148	1.119	1.103	1.046	0.99
3	1.197	1.255		1.304	1.311		1.309	1.284	1.276		1.218	1.181		1.085	1.00
4	1.204	1.253	1.313	1.337	1.341	1.354	1.331		1.298	1.287	1.263	1.212	1.162	1.083	1.013
5	1.211	1.264	1.332	1.372		1.324	1.280	1.285	1.248	1.259		1.242	1.177	1.090	1.017
6	1.219	1.290		1.378	1.338	1.280	1.237	1.225	1.205	1.213	1.239	1.243		1.109	1.019
7	1.215	1.271	1.356	1.370	1.307	1.251	1.247	1.262	1.214	1.184	1.204	1.231	1.189	1.087	1.009
8	1.209	1.250	1.346		1.328	1.254	1.277		1.243	1.184	1.218		1.174	1.080	0.994
9	1.214	1.271	1.357	1.371	1.308	1.251	1.246	1.260	1.210	1.178	1.194	1.217	1.172	1.067	0.980
10	1.218	1.290		1.381	1.340	1.280	1.236	1.220	1.196	1.199	1.216	1.214		1.069	0.974
11	1.210	1.265	1.335	1.376		1.327	1.279	1.278	1.235	1.238		1.202	1.126	1.032	0.949
12	1.203	1.256	1.319	1.344	1.367	1.358	1.331		1.283	1.261	1.225	1.160	1.096	1.004	0.919
13	1.198	1.261		1.315	1.322		1.311	1.278	1.260		1.174	1.119		0.983	0.885
14	1.185	1.222	1.262	1.253	1.253	1.263	1.226	1.182	1.174	1.159	1.106	1.050	1.007	0.921	0.832
15	1.179	1.189	1.204	1.204	1.201	1.194	1.170	1.141	1.116	1.086	1.041	0.990	0.933	0.856	0.764

Figure 2

ASSEMBLY C 11 BOL POWER DISTRIBUTION

	R	P	N	M	L	K	J	H	G	F	E	D	C	B	A
1	1.185	1.196	1.211	1.215	1.219	1.224	1.216	1.206	1.206	1.205	1.192	1.179	1.168	1.148	1.133
2	1.195	1.232	1.273	1.269	1.275	1.296	1.273	1.246	1.262	1.274	1.243	1.226	1.223	1.175	1.132
3	1.210	1.273		1.292	1.346		1.360	1.343	1.346		1.309	1.283		1.206	1.137
4	1.212	1.266	1.331	1.360	1.391	1.391	1.376		1.361	1.364	1.347	1.304	1.264	1.191	1.129
5	1.215	1.272	1.344	1.369		1.354	1.316	1.329	1.299	1.321		1.325	1.268	1.187	1.121
6	1.218	1.291		1.388	1.353	1.299	1.263	1.257	1.245	1.263	1.298	1.315		1.194	1.110
7	1.208	1.266	1.354	1.371	1.313	1.261	1.263	1.285	1.244	1.222	1.251	1.289	1.256	1.158	1.086
8	1.196	1.238	1.336		1.325	1.255	1.283		1.261	1.210	1.254		1.225	1.116	1.058
9	1.194	1.251	1.337	1.353	1.294	1.241	1.241	1.260	1.216	1.190	1.215	1.247	1.210	1.110	1.037
10	1.190	1.261		1.352	1.314	1.259	1.219	1.208	1.190	1.199	1.224	1.232		1.100	1.011
11	1.174	1.220	1.296	1.337		1.292	1.248	1.252	1.215	1.224		1.203	1.137	1.048	0.972
12	1.158	1.208	1.269	1.294	1.317	1.369	1.285		1.247	1.232	1.203	1.147	1.090	1.006	0.930
13	1.144	1.203		1.253	1.269		1.253	1.224	1.210		1.138	1.091		0.971	0.881
14	1.186	1.154	1.191	1.180	1.180	1.190	1.156	1.116	1.112	1.102	1.050	1.007	0.972	0.896	0.817
15	1.096	1.108	1.121	1.119	1.115	1.108	1.086	1.060	1.040	1.015	0.976	0.933	0.885	0.818	0.737

Figure 3

ASSEMBLY B9 EOL POWER DISTRIBUTION

	R	P	N	M	L	K	J	H	G	F	E	D	C	B	A
1	1.241	1.241	1.250	1.253	1.256	1.259	1.252	1.243	1.241	1.237	1.223	1.207	1.191	1.165	1.141
2	1.240	1.256	1.283	1.279	1.284	1.298	1.281	1.241	1.269	1.275	1.249	1.231	1.221	1.177	1.135
3	1.250	1.282		1.321	1.331		1.338	1.325	1.325		1.294	1.270		1.199	1.138
4	1.253	1.279	1.321	1.341	1.361	1.359	1.348		1.334	1.332	1.320	1.287	1.252	1.190	1.135
5	1.256	1.285	1.332	1.361		1.335	1.306	1.312	1.291	1.305		1.302	1.256	1.189	1.131
6	1.240	1.300		1.361	1.336	1.296	1.269	1.261	1.251	1.263	1.287	1.296		1.197	1.125
7	1.255	1.285	1.341	1.352	1.310	1.269	1.267	1.280	1.250	1.234	1.255	1.280	1.251	1.172	1.109
8	1.248	1.267	1.331		1.319	1.266	1.284		1.264	1.227	1.258		1.232	1.143	1.090
9	1.249	1.279	1.335	1.345	1.302	1.261	1.257	1.268	1.236	1.217	1.235	1.256	1.224	1.142	1.076
10	1.249	1.269		1.348	1.321	1.279	1.247	1.237	1.223	1.229	1.246	1.248		1.136	1.058
11	1.240	1.269	1.315	1.342		1.309	1.276	1.276	1.248	1.253		1.232	1.176	1.099	1.029
12	1.232	1.258	1.299	1.317	1.332	1.326	1.308		1.277	1.264	1.240	1.194	1.143	1.067	0.996
13	1.224	1.256		1.290	1.296		1.289	1.267	1.255		1.195	1.153		1.041	0.957
14	1.209	1.223	1.247	1.240	1.240	1.247	1.222	1.190	1.184	1.173	1.129	1.089	1.053	0.980	0.902
15	1.201	1.194	1.200	1.198	1.195	1.190	1.173	1.151	1.132	1.109	1.073	1.031	0.982	0.915	0.833

Figure 4

ASSEMBLY C11 EOL POWER DISTRIBUTION

	R	P	N	M	L	K	J	H	G	F	E	D	C	B	A
1	1.191	1.190	1.199	1.202	1.205	1.208	1.203	1.195	1.195	1.194	1.183	1.172	1.161	1.140	1.132
2	1.189	1.209	1.229	1.225	1.230	1.244	1.228	1.210	1.220	1.227	1.205	1.191	1.184	1.147	1.110
3	1.197	1.228		1.269	1.273		1.280	1.269	1.270		1.244	1.224		1.163	1.109
4	1.199	1.223	1.262	1.281	1.299	1.298	1.287		1.276	1.276	1.266	1.236	1.205	1.150	1.101
5	1.201	1.226	1.270	1.298		1.272	1.295	1.251	1.232	1.246		1.247	1.206	1.145	1.092
6	1.202	1.239		1.296	1.271	1.232	1.295	1.199	1.190	1.203	1.227	1.237		1.147	1.083
7	1.195	1.222	1.275	1.284	1.243	1.204	1.201	1.213	1.185	1.171	1.193	1.217	1.192	1.120	1.063
8	1.186	1.202	1.263		1.248	1.197	1.212		1.195	1.160	1.191		1.169	1.087	1.039
9	1.185	1.211	1.263	1.271	1.228	1.188	1.189	1.194	1.163	1.146	1.164	1.185	1.156	1.081	1.021
10	1.182	1.217		1.270	1.242	1.200	1.169	1.159	1.145	1.152	1.169	1.172		1.070	0.999
11	1.170	1.194	1.235	1.259		1.224	1.191	1.190	1.164	1.169		1.151	1.100	1.030	0.966
12	1.157	1.179	1.215	1.230	1.242	1.235	1.216		1.185	1.173	1.151	1.109	1.063	0.993	0.929
13	1.145	1.172		1.199	1.202		1.191	1.170	1.157		1.102	1.064		0.963	0.887
14	1.124	1.134	1.154	1.144	1.142	1.146	1.120	1.089	1.083	1.073	1.032	0.995	0.964	0.898	0.829
15	1.105	1.099	1.101	1.097	1.091	1.084	1.065	1.043	1.025	1.004	0.970	0.933	0.890	0.830	0.758

Figure 5

ATTACHMENT II

REVISION TO TECHNICAL SPECIFICATION

H. B. ROBINSON UNIT 2, CYCLE 2

August 15, 1973

3.10.1.5 During physics and control rod exercises, the insertion limits need not be observed, but the Figure 3.10-2 must be observed.

3.10.2 Power Distribution Limits

3.10.2.1 Limiting Values

3.10.2.1.1 Power distribution limits are expressed as hot channel factors.

Limiting values above 94.8% rated power are:

$F^N_{\Delta H} = 1.55 \{1 + 0.2 (1 - P)\}$

$F^N_q = 2.34/P$ for Regions 2 and 3 fuel

$F^N_q = 2.49/P$ for Region 4 fuel

where P is the fraction of rated power at which the core is operating ($P < 1.0$).

If measured peaking factors exceed these values with due allowance for measurement error, the maximum allowable power level shall be reduced in direct proportion to the amount which F^N_q or $F^N_{\Delta H}$ exceed the limiting values, whichever is more restrictive.

3.10.2.1.2 At all times the hot channel factors, as defined in the basis, must meet the following limits:

$F^N_q \leq 2.52 \{1 + 0.2 (1 - P)\}$ in the indicated flux difference range -17 to +9%

$F^N_{\Delta H} \leq 1.55 \{1 + 0.2 (1 - P)\}$

where P is the fraction of rated power at which the core is operating ($P < 1.0$).

If measured peaking factors exceed these values with due allowance for measurement error, the maximum allowable reactor power level and the nuclear overpower trip setpoint shall be reduced in direct proportion to the amount which F^N_q or $F^N_{\Delta H}$ exceed the limiting valves, whichever is more restrictive. If the hot channel factors cannot be reduced below the limiting valves within twenty-four hours, the overpower ΔT and overtemperature ΔT trip setpoint shall be similarly reduced.

(3)

3.10.2.2 During surveillance of the axial peaking factor, which occurs above 94.8% rated power, the nuclear hot channel factor, F_q^N, during Cycle 2 shall be determined by

$$F_q^N = \overline{R}\ (1 + \sigma) \cdot F_q^a \cdot (F(z)\ S(z)) \cdot F_u^N \cdot \{1 + 2\ (T - 0.02)\}$$

where

$\overline{R}$ is a thimble dependent factor derived from at least six of the most current full incore power maps which relates the Fz measured in a given thimble to F_q^N.

σ is the standard deviation associated with the determination of $\overline{R}$.

F_q^a is the uncertainty associated with the analog equipment used to determine the product F(z) S(z). A value of 1.02 is appropriate. (3)

F(z) S(z) = the value of the core axial peak to average power as determined by the product of the densification penalty factor S(z) as a function of core height and the corresponding value of the average core axial point-to-average power F(z) from the incore movable detector system. S(z) is defined in Figure 3.10-3, and includes the variation of limiting kW/ft as a function of core height above the core midplane. (3)

F_u^N = the value of the nuclear uncertainty factor, or uncertainty in knowledge of the nuclear peaking factor. It is the measurement uncertainty associated with a result obtained from a full-core flux map with the movable detectors. A value of 1.05 is appropriate.

T = the peak quadrant power relative to the average of the four quadrants as determined by the excore nuclear instrumentation, having a value up to 1.10.

The value of F_q^N less than or equal to 2.34 for Regions 2 and 3 and 2.49 for Region 4 is consistent with operation at rated power, as outlined in Section 5.4 of WCAP-8114. (3)

Axial surveillance of F_z^N during Cycle 2 shall consist of:

(a) Traverses with the movable incore detectors in appropriate pairs of detector paths shall be taken every eight hours, or a frequency of approximately 0, 10, 30, 60, 120, 180, 240, 360, and 480 minutes following accumulated control rod motion in any one direction of five steps or more, exclusive of control rod movements within 15 steps from the top of the core. From the traverses, determination of F(z) S(z) shall be made and shown to result in an F_q^N less than the value specified in 3.10.2.1. (3)

(b) Axial surveillance shall not be required below 94.8 power.

(c) Surveillance limits on F(z) S(z) will be based on the most limiting core region, assuring that all F_q^N limits will be met. (3)

3.10.2.3 During periods when surveillance of the axial peaking factor in accordance with Specification 3.10.2.2 is not in effect, the nuclear hot channel factor, F_q^N, during Cycle 2 shall be determined by

$$F_q^N = \overline{R}\ (1 + \sigma) \cdot F_q^a \cdot (F(z) \cdot S(z) \cdot F_u^N \cdot (1 + 2\ (T - 0.02))$$

where

$\overline{R}$, σ, F_q^a, F(z), and S(z) are as defined in Section 3.10.2.2 and are determined based on a movable incore detector map taken on at least a monthly basis. The value of F_q^N less than or equal to 2.52 is consistent with operation at 94.8% rate power as outlined in Section 5.4 of WCAP-8114. (3)

3.10.2.4 At or above 94.8% rated power the indicated axial flux difference must be maintained within the range +9% to -17%. For every 3.5% below 94.8% rated power level, the permissible positive flux difference range is extended by +1 percent. For every 2% below 94.8% rated power level, the permissible negative flux difference range is extended by -1 percent. (3)

shapes, including the effects of fuel densification, are not exceeded if the axial offset (flux difference) is maintained between -20 and +12%. The specified limits of -17 and +9% allow for a 3% error in the axial offset. Therefore, there is no requirement for measurement where the LOCA limited peak local rod power corresponds to an $F_q^N \leq 2.52$ (94.8% rated power) providing the flux difference is maintained between -20, +12%. For operation at a fraction, P, of rated power, design limits are met provided, (3)

$$F_{\Delta H}^N \leq 1.55 \quad \{1 + 0.2\ (1-P)\}$$

$$F_q^N \leq 2.52 \quad \{1 + 0.2\ (1-P)\}$$ in the indicated flux difference range -17% to +9% (3)

The permitted relaxation allows radial power shape changes with rod insertion to the insertion limits. It has been determined that provided the above conditions 1 through 5 are observed, these hot channel factors limits are met.

For normal operation and anticipated transients the core is protected from exceeding the fuel centerline melt limit, or 18.6 kW/ft locally, and from going a minimum DNBR of 1.30, by automatic protection on power, flux difference, pressure and temperature. Only conditions 1 through 4, above, are mandatory since the flux difference is an explicit input to the protection system. (3)

For operation above 94.8% rated power, additional core surveillance is required as an F_q^N of 2.52 is no longer adequate to meet LOCA linear heat generation rate limits. At full power, these limits are:

$$F_q^N \leq 2.34 \quad \text{for Regions 2 and 3 fuel}$$

$$F_q^N \leq 2.49 \quad \text{for Region 4 fuel}$$

If it is determined that these limits are violated, a proportional reduction in power level will continue to satisfy the linear heat generation rate limits of 14.2 kW/ft and 15.1 kW/ft. Additional core surveillance will consist of monitoring of the axial power shape either manually or with an automatic system utilizing selected thimbles of the movable incore detector system. Limiting values of the axial power shape will be determined such that the limits of F_q^N will not be violated, as specified in Section 3.10.2.2. (3)

Measurements of the hot channel factors are required as part of startup physics tests and whenever abnormal power distribution conditions require a reduction of core power to a level based on measured hot channel factors.

In the specified limit of F_q^N there is a 5% allowance for uncertainties(1) which means that normal operation of the core within the defined conditions and procedures is expected to result in a measured $F_q^N \leq 2.34/1.05$ for Regions 2 and 3, for example, at rated power even on a worst case basis. When a measurement is taken experimental error must be allowed for and 5% is the appropriate allowance for a full core representative map taken with the movable incore detector flux mapping system. (3)

The measured value of F_q^N must be additionally corrected by including a penalty as shown on Figure 3.10-3 (at the appropriate core location) to account for fuel densification effects before comparison with the limiting value above.

In the specified limit of $F_{\Delta H}^N$ there is an 8% allowance for design prediction uncertainties, which means that normal operation of the core is expected to result in $F_{\Delta H}^N \leq 1.55/1.08$ at rated power. The uncertainty to be associated with a measurement of $F_{\Delta H}^N$ by the movable incore system on the other hand, is 3.65%, which means that the normal operation of the core shall result in a measured $F_{\Delta H}^N \leq 1.55/1.0365$ at rated power. The logic behind the larger design uncertainty in this case is that (a) abnormal perturbation in the radial power shape (e.g. rod misalignment) affect $F_{\Delta H}^N$, is in most cases without necessarily affecting F_q^N, through movement of part length rods, and can limit it to the desired value, (b) while the operator has some control over F_q^N through F_z^N by motion of control rods, he has no direct control over $F_{\Delta H}^N$, and (c) an error in the predictions for radial power shape, which may be detected during start-up physics tests can be compensated for in F_q^N by tighter axial control, but compensation for $F_{\Delta H}^N$ is less readily available.

FIGURE 3.10-3

POWER SPIKE VS ELEVATION

H.B. ROBINSON UNIT 2 - CYCLE 2

INCLUDES EFFECT OF VARIABLE KW/FT LIMIT